

Human Entesis Group 3 Innate Lymphoid Cells

Richard J Cuthbert¹ (BSc, PhD), Evangelos M. Fragkakis^{1,2} (MD, MDres.), Robert Dunsmuir² (BSc Hons, MB, ChB, FRCS Ed, Frcs Orth), Zhi Li³ (MSc, PhD), Mark Coles³ (BSc, PhD), Helena Marzo-Ortega^{1,4} (LMS, MRCP, PhD), Peter Giannoudis¹ (MD, FACS, FRCS), Elena Jones¹ (PhD), Yasser M El-Sherbiny^{1,4,5} (PhD), Dennis McGonagle^{1,4*} (PRCPI, PhD).

¹Leeds Institute of Rheumatic and Musculoskeletal Medicine, University of Leeds, Leeds, United Kingdom.

²Department of Spinal Surgery, The Leeds teaching hospitals NHS trust, Leeds, United Kingdom.

³Centre for Immunology and Infection, University of York, York, United Kingdom.

⁴NIHR-Leeds Musculoskeletal and Biomedical Research Unit, Chapel Allerton, Leeds Teaching Hospital Trust, Leeds, West Yorkshire, UK.

⁵Clinical pathology department, Mansoura University Hospitals, Mansoura University, Mansoura, Egypt.

***Corresponding author: Dennis McGonagle**

Wellcome trust Brenner Building, St James's University Hospital, Becket Street, Leeds, LS97TF

Tel: +44 7817 407699

E-mail: D.G.McGonagle@leeds.ac.uk

Financial support

This work was supported in part by a Pfizer Ltd. investigator initiated research grant.

Competing financial interests

The Authors have no competing financial interests

ABSTRACT

Objective

Group 3 innate lymphoid cells (ILC3s) play a pivotal role in barrier tissues such as the gut and the skin, two important sites of disease in spondyloarthritis (SpA). It was investigated whether normal and injured human enthesis, the key target tissue in early SpA, harboured ILC3s in enthesal soft tissue (EST) and adjacent peri-enthesal bone (PEB).

Methods

Interspinous ligament and spinous process bone was collected from donors with no systemic inflammatory disease, enzymatically digested and immunophenotyped. The immunological profile of enthesal cells was examined and the transcriptional profile of sorted ILC3s was compared to those isolated from SpA synovial fluid. To assess the ability of enthesal tissue to produce IL-17 and IL-22 enthesal digests were stimulated with IL-23 and IL-1 β . Osteoarthritic and ruptured Achilles tissue was examined histologically.

Results

Compared to peripheral blood, human EST had a higher proportion of ILCs ($p=0.008$), EST and PEB both had a higher proportion of NKp44⁺ ILC3s ($p=0.001$ and $p=0.043$). *ROR γ t*, *STAT3* and *IL-23R* transcript expression validated the enthesal ILC3 phenotype. Cytokine transcript expression was similar in ILC3s isolated from enthesis and SpA synovial fluid. Normal enthesal digests stimulated with IL-23/IL-1 β upregulated *IL17A* transcript and histological examination of injured/damaged entheses showed ROR γ t expressing cells.

Conclusion

This work shows that human enthesis harbours a resident population of ILC3s, with the potential to participate in spondyloarthritis pathogenesis.

INTRODUCTION

There is increasing evidence that the enthesis organ and biomechanically related structures may be an important site for disease initiation in spondyloarthritis (SpA) (1, 2). In animal models, including IL-23 and TNF α overexpression systems, primary enthesal disease results in subsequent spreading to the adjacent synovium and bone (1, 3). Until recently, the enthesis with its avascular region of fibrocartilage at the bone interface and adjacent tendon, ligament or capsules that are composed of fibrocartilage and dense stromal connective tissue was not studied as an immune organ. However, the seminal work of Sherlock and colleagues showed that the normal murine enthesis had a low abundance of immune cells that were IL-23 dependent that are nevertheless, critical to SpA pathogenesis (1).

The description of a family of cytokine dependent innate lymphoid cells (ILCs), that play a pivotal role in barrier tissue homeostasis, repair and inflammation (4, 5) has led to major new avenues for inflammatory disease immunopathogenesis investigation. In recent years, the importance of ILCs in gut and skin, both targets of SpA in man, has been reported with a possible role for these cells in tissue repair and homeostasis (4, 5). Since the normal mechanically stressed human enthesis is a site of microdamage and microscopic inflammation in normal aged enthesis, it is feasible that the human enthesis under physiological conditions may also contain ILCs.

In humans, ILCs can be broadly subdivided into three main categories; ILC1s which are defined by their ability to produce IFN γ , ILC2s that are able to produce T_H2 associated cytokines and an ILC3 subpopulation characterised by expression of the truncated retinoic acid-receptor (RAR)-related orphan receptor gamma (ROR γ t) (5). Human SpAs are genetically linked to the IL-23/17 cytokine axis (6) and therapeutic antagonism of this pathway is effective in SpA (6) the ability of ILC3s to respond to IL- β / IL-23 signalling with IL-17 and IL-22 production is especially relevant (5). Additionally, ILC3s are comparatively abundant in SpA related synovial fluid (7, 8) and have also been shown to be increased in psoriatic skin (9) and play a pivotal role in gut homeostasis and in experimental inflammatory bowel disease (4, 5, 7). Given the importance of ILC3 in the skin and gut in addition to emerging animal model data, we hypothesised that the normal human enthesis harbours ILC3s with the potential for activation by local or systemic IL-23. Herein, we describe methodology for the assessment of human enthesal immune populations in health and following immune stimulation and provide a preliminary characterisation of human group 3 ILCs.

METHODS

Enthesis samples.

Normal inter-spinous process enthesis (n=13, median age 52, 8 male) were obtained from patients undergoing spinal decompression, or scoliosis correction surgery of thoracic or lumbar vertebrae. Unmatched peripheral blood was also collected both from patients undergoing surgery and from healthy controls (n=14, median age 42, 9 male). To compare normal enthesal ILC3s with those from active inflammatory disease, synovial fluid samples from knee synovitis in SpA were also examined (n=4).

To determine whether ILCs might be present at sites of entheses damage, injured entheses was obtained from patients undergoing surgical repair of ruptured Achilles' tendons with tissue being procured from the peri-enthesal rupture site (n=3). Similarly, anterior cruciate ligament (ACL), which is known to be damaged by the osteoarthritic process, was obtained from patients undergoing knee arthroplasty for the treatment of advanced osteoarthritis (n=7).

Digested Enthesis Immune cell cytometric evaluation.

Since the earliest lesions in human SpA appear to occur in either the entheses soft tissue or in sub-fibrocartilagenous bone (10), both Enthesal soft tissue (EST) and peri-enthesal bone (PEB) was initially separated, see Figure 1A and digested in collagenase solution as previously described (11), for a detailed description see supplementary methods. Mononuclear cells were isolated using a density gradient medium, LymphoprepTM (Axis Shield, Dundee, UK) in all cases. T-cells, B-cells and natural killer cells (NK cells) were discriminated based on forward and side scatter characteristics and expression of CD45 then CD3, CD19 and CD56 respectively. T-cell subsets, T-helper cells and cytotoxic T-cells were discriminated based on expression of CD4 and CD8 respectively, T-cells that did not express CD4 or CD8 (CD4^{neg}CD8^{neg}) were also measured and $\gamma\delta$ T-cell were identified based on expression of T-cell receptor (TRC) $\gamma\delta$ (Supplementary Figure 1). Enthesal ILC subsets were discriminated based on expression of cell surface phenotype; ILC1: Lin⁻ (CD1a, CD3, CD14, CD11c, CD19, CD34, CD94, CD123, CD303, FC ϵ R1, TRC $\alpha\beta$, TRC $\gamma\delta$) CD45⁺, CD127⁺, CRTH2⁻, c-Kit⁻. ILC2: Lin⁻, CD127⁺, CD45⁺, CRTH2⁺. ILC3: Lin⁻, CD45⁺, CD127⁺, CRTH2⁻, c-Kit⁺ (5, 7, 8) (Supplementary Table 1), dead cells were discriminated based on uptake of aqua dye (ThermoFisher, Altrincham, UK), or 7-Amino actinomycin D (BD, Oxford, UK). An Influx (BD) fluorescence activated cell sorter was used to isolate enthesal ILC subsets, immunophenotyping in unsorted samples was performed on a LSR II flow cytometer (BD).

Transcript analysis pre and post enthesal digest cytokine stimulation.

Analysis of key IL-23/IL-17 axis cytokine expression changes was performed on unsorted whole enthesal digests. Following digestion, 2×10^6 cells were incubated at 37°C, 5% CO₂ with Iscove's Modified Dulbecco's Medium (Gibco, Paisley, UK) containing 10% foetal calf serum (Biosera, Boussens, France) in the presence or absence of IL-1 β (10ng/ml, Miltenyi Biotec, Bisley, UK) and IL-23 (50ng/ml, Miltenyi), after 48 hours cells were prepared for RNA isolation.

RNA was isolated using PicoPure RNA isolation kit (ThermoFisher), and cDNA was synthesised using a high capacity reverse transcription kit (ThermoFisher). Pre-amplification of target transcripts was performed using GE PreAmp kit (Fluidigm, San Francisco, USA), this step was omitted in cytokine stimulation assays. Quantitative real-time PCR was performed using an ABI7500 (Applied Biosystems) thermocycler to measure expression of immunomodulatory and pro-inflammatory transcripts. All target gene expression was calculated relative to expression of housekeeping gene *HPRT1*, values below detection were not considered or plotted unless otherwise stated.

Histology and Immunofluorescence microscopy.

For immunofluorescence microscopy, frozen sections of healthy enthesal soft tissue (EST) were incubated with fluorescently labelled antibodies against CD3 and ROR γ t (Supplementary Table 1) and counterstained with 4',6-Diamidino-2'-phenylindole dihydrochloride (DAPI).

Tissue samples from Achilles' tendon, ACL (Figure 1B) and spinous process were prepared for histology using standard protocols and stained using mouse anti-human ROR γ t (Supplementary Table 1), EnVision+ horseradish staining system (Dako, Ely, UK) and counterstained with Harris haematoxylin.

Statistics

The Independent samples Kruskal-Wallis Test was used to detect differences between peripheral blood, EST and PEB samples with regards to the proportions of T-cells and cells classified as "others" in Figure 1C as well as CD4^{neg}CD8^{neg} T-cells and $\gamma\delta$ T-cells in Figure 1D. The Wilcoxon Signed Rank Test was used to detect changes in gene expression in enthesal digests with or without cytokine stimulation. The Mann-Whitney U test was used to detect difference between groups in all other data sets. Significance was set at >95%, SPSS version 21 (IBM) was used to calculate all statistics, GraphPad Prism 6 (GraphPad Software) was used to generate all graphs. Bar charts show mean and standard error, box plots show median (line), interquartile range (box) and extreme values (whiskers).

RESULTS

Immunological profiling of enthesal tissue

Initial assessment of the total enthesal lymphocyte content revealed significant differences in the proportions of T-cells between aged-matched peripheral mononuclear cells (PBMCs) and EST and PEB digests ($p=0.018$). There was also a significant difference in the percentage of cells not defined as T-cells, B-cells or NK-cells within these categories ($p=0.016$, Figure 1C). Examination of T-cell subsets also showed an increase in the proportion of T-cells expressing neither the CD4 or CD8 antigen in enthesal digests compared to peripheral blood ($p=0.021$). Additionally, $\gamma\delta$ T-cells were also significantly increased in comparison to peripheral blood ($p=0.027$, Figure 1D).

ILC3s defined as Lin⁻, CD45⁺, ROR γ t⁺, CD3⁻ were not detected in the normal enthesal tissue using immunofluorescence, likely reflecting their extreme rarity in health (Supplementary Figure 2), necessitating a cytometric approach to ILC3 detection. Digested enthesal tissue showed the consistent presence of ILCs as identified by cell surface phenotype (Figure 1E) (5).

ILCs detected in enthesal tissues have a distinct phenotype from those in peripheral blood

In order to ascertain if ILCs detected in enthesal tissues were a resident population, as distinct from passenger cells merely trapped in the vasculature, the frequency of all ILCs in peripheral blood was compared to EST and PEB digests. EST had a substantially greater proportion of ILCs ($p=0.008$) compared to unmatched peripheral blood median 0.08% (0.03-0.20%), EST: 0.54% (0.06-2.06%), PEB: 0.24% (0.03-0.49%, Figure 1F). The proportion of total ILCs identified as ILC3 and expressing the NKp44 cell surface antigen was also examined. In peripheral blood, the percentage of lymphocytes identified as ILC3s and expressing the NKp44 marker was 0.21% (0-1.13%) EST digests had a significantly greater proportion of these cells, median 5.3% (0.8-50.9%, $p=0.001$). These were also elevated in PEB digests, median 3.03% (0-13.84%, $p=0.043$) compared to peripheral blood (Figure 1G). Taken together these data provide strong evidence that the ILC3 populations in EST and PEB tissue are enthesal resident and unlikely to originate from peri-enthesal blood vessels. In EST ILC3s constituted 0.25% (0.02-0.92%) of the total lymphocyte population. NKp44⁻ ILC3s constituted 0.16% (0.01-0.17%) and those expressing the NKp44 marker constituted 0.09% (4.25×10^{-3} -0.23%). Cells phenotypically identified as ILC1s constituted 0.20% (0-0.49), ILC2s 0.23% (0-1.17%) of the total lymphocytic fraction (Supplementary Table 2). The proportion of ILC subsets observed in PEB was broadly similar to EST; PEB did contain fewer ILC2s on average although this was not statistically significant.

Confirmation of ILC3 phenotype and comparison to synovial SpA origin ILC3s

Comparison of gene expression from ILC3s sorted from EST showed a highly significant increase in the expression of *RORC* (*RORγt*) transcript compared to unsorted enthesal derived mononuclear cells ($p=0.009$, Figure 2A) confirming ILC3 phenotype (5). Similar results were obtained from ILC3s isolated from PEB ($p=0.032$, Figure 2B). Since the frequency of ILC3s is known to be increased in the synovial fluid of patients suffering from SpA (7), comparison of immunomodulatory transcripts from ILC3s isolated from enthesis and SpA synovial fluid was made to further confirm ILC3 phenotype. Sorted ILC3 transcript analysis showed high expression of *TGFβ* and *TNFα*, both mediators with opposing immunomodulatory and inflammatory roles in the context of SpA respectively (12). *STAT3* was expressed in all tissues indicating potential for cytokine signal transduction but significantly higher level in PEB ILC3s compared to both EST and SpA synovial fluid ILC3s ($p=0.048$, Figure 2C). Expression of IL-10 in ILC3s from three of five EST was noted and two of five PEB and SpA tissues, The EST ILC3s had no detectable *IL-17A* or *IL-22*; however, *IL-17A* message was detected in ILCs in two of five samples from normal PEB and in one of four samples from SpA synovial fluid. *IL-22* message was detected in one sample from both PEB and SpA synovial fluid (data not shown). In general, transcript expression between ILC3 isolated from enthesis tissues and SpA fluid was similar, strengthening the proposition that these cells share common functionality.

Cytokine Stimulation of Enthesis

Examination of IL-23R expression from ILC3 isolated from either EST or PEB showed a significantly increased level of *IL-23R* transcript compared to unsorted mononuclear cells ($p=0.033$, Figure 2D) both confirming immunophenotype data and the capacity for IL-23 responsiveness in these cells.

Transcriptional analysis of IL-1β/IL-23 cytokine stimulated enthesal digests showed a significant

increase ($p=0.046$) in expression of *IL-17A* (Figure 2E). Expression of *IL-17F* and *IL-22* also showed a clear upward trend following stimulation although this fell short of significance (Figures 2F and 2G). These data provide functional support for human enthesal resident cells capable of *IL-17A* production in response to cytokine stimulation.

Evidence for ILC3s at sites of Enthesis Injury

Tissue from peri-enthesal regions of ruptured tendons showed inflammatory infiltrates expressing the ROR γ t protein this was observed in 2 of 3 donors (Figure 3A). Likewise, peri-enthesal tissue from intact ACL from osteoarthritic donors showed cells expressing the ROR γ t protein in enthesal soft tissue in 5 of 7 donors (Figure 3B) and in the peri-enthesal bone 7 of 7 donors (Figure 3C). Positive staining for ROR γ t was also observed in areas of active bone re-modelling in OA in 5 of 7 donors (Figure 3D). For comparison, healthy spinal tissue was also examined. Positive staining was absent in 6 of 7 of EST tissues (Figure 3E) as well as in control Achilles tendon (data not shown). Expression ROR γ t was observed in control PEB, harvested from spinous process (Figure 3E), and consistently present in cancellous bone harvested from iliac crest (data not shown).

DISCUSSION

Recently there has been a convergence of genetic, molecular and therapeutic data pointing towards a role for the *IL-23/17* axis in the pathogenesis of the SpA group of related diseases including psoriasis and inflammatory bowel disease. With the expanding literature showing that group 3 ILCs play an important role in skin and gut homeostasis, we investigated whether ILC3s were present at the human enthesis a key target tissue in early SpA. The proportion of ILC3s expressing the NKp44 marker in enthesal soft tissue and peri-enthesal bone confirms that these cells are resident populations of ILCs and could not entirely be made-up cells released from peripheral blood vessels.

To confirm our phenotypic evaluation, ROR γ t transcript was measured in sorted ILC3s and found elevated ROR γ t transcript levels, an important ILC3 lineage transcription factor (4). The detection of *IL-23R* transcripts in ILC3 isolates gives additional confirmation of ILC3 phenotypes. Abundant TGF β was found in normal enthesal ILC3s, possibly indicating an immunoregulatory phenotype in the absence of inflammatory signalling. However, TGF β was also elevated in ILCs from SpA synovial fluid, a known inflammatory environment (7). Overall, ILC3s isolated from enthesal tissues and SpA synovial fluid were very similar in their expression of cytokine transcripts perhaps indicating comparable activation states. It should be noted that in this study transcriptional analysis was limited due to the low cellular yield from sorted populations. Indeed, in many cases conventional PCR was unable to resolve the expression levels of some genes of interest. Ultra-low cell number or single cell compatible techniques such as RNAseq may provide a more appropriate means of characterising enthesal populations in future.

Normal whole enthesal digests were stimulated with *IL-1 β* and *IL-23* and showed a clear increase in *IL-17* and, to a lesser extent, *IL-22* transcripts. Although this work does not address the cellular origin

of these signals it nevertheless confirms that this relatively acellular tissue is capable of responding as a whole to stimulation by increasing *IL-17* and *IL-22* transcript production. ROR γ t transcription factor expression was found in inflammatory infiltrate of ruptured Achilles tendon tissue and in peri-enthesal bone in OA derived entheses. Although it is likely that cells other than ILC3s, including Th17 cells, contribute a large portion of this signal this nevertheless highlights the involvement of the IL-23/IL-17 axis in responding to injury at the entheses.

The elevated proportion of NKp44⁺ ILC3s is interesting from a functional perspective since it has been shown that NKp44 positive but not negative ILC3s are capable of producing IL-22 (5). Given that IL-22 signalling has been implicated in promoting osteogenesis (13), the presence of an elevated proportion of NKp44⁺ ILC3s may suggest a potential mechanism for spondyloarthropathy pathogenesis in respect to new bone formation.

The present studies in man was motivated by the emerging literature on ILCs and from the IL-23 dependent model of SpA reported by Sherlock et al (1). Recent murine model studies have shown that this IL-23 SpA model is associated with an accumulation of $\gamma\delta$ T-cells in enthesal regions (14). These T-cells do not typically express CD4 or CD8 and share many similarities to ILC3s, particularly in their response to cytokine stimulation. Although some caution should be given to direct comparison between animal models and human disease, we noted that T-cells that lacked expression of CD4 and CD8 were elevated in enthesal digests. Further examination of T-cell subsets indicated that a high proportion of these cells were likely $\gamma\delta$ T-cells, further characterisation of this T-cell subset in human entheses is important especially in light of the animal model data suggesting a role for $\gamma\delta$ T-cells in SpA pathogenesis (1, 14).

In conclusion, this proof of concept work demonstrated that entheses related soft tissue and peri-enthesal bone harbours a population of resident ILC3s. The frequency of such cells as a proportion of CD45⁺ lymphocytes is marginally lower (0.25% in EST, 0.07% in PEB) than that reported in gut (~0.90%) (15) and skin (0.35%) (9). This lower frequency may be due to entheses non-exposure to external environments compared to the skin and gut. Further work is needed to define the exact micro-anatomical topography of these rare cells and to look at other entheses around the body, as well as to undertake studies in disease. The ability to robustly define and purify these rare cells and define other immune cells at the enthesopathies opens up new avenues to explore immunity in early SpA.

Acknowledgements

We would like to acknowledge Adam Davison and Elizabeth Straszynski for the expert flow cytometry support provided throughout this study. This research is supported by the National Institute for Health Research (NIHR) Leeds Musculoskeletal Biomedical Research Unit. The views expressed are those of the author(s) and not necessarily those of the NHS, the NIHR or the Department of Health.

References

1. Sherlock JP, Joyce-Shaikh B, Turner SP, Chao CC, Sathe M, Grein J, et al. IL-23 induces spondyloarthritis by acting on ROR-gamma+ CD3+CD4-CD8- enthesal resident T cells. *Nat Med*. 2012 Jul;18(7):1069-76. PubMed PMID: 22772566.
2. McGonagle D, Gibbon W, Emery P. Classification of inflammatory arthritis by enthesitis. *The Lancet*. 1998;352(9134):1137-40.
3. Armaka M, Apostolaki M, Jacques P, Kontoyiannis DL, Elewaut D, Kollias G. Mesenchymal cell targeting by TNF as a common pathogenic principle in chronic inflammatory joint and intestinal diseases. *J Exp Med*. 2008 Feb 18;205(2):331-7. PubMed PMID: 18250193. Pubmed Central PMCID: 2271010.
4. Spits H, Di Santo JP. The expanding family of innate lymphoid cells: regulators and effectors of immunity and tissue remodeling. *Nature immunology*. 2011 Jan;12(1):21-7. PubMed PMID: 21113163.
5. Spits H, Artis D, Colonna M, Dieffenbach A, Di Santo JP, Eberl G, et al. Innate lymphoid cells—a proposal for uniform nomenclature. *Nature Reviews Immunology*. 2013;13(2):145-9.
6. Fragoulis GE, Siebert S, McInnes IB. Therapeutic Targeting of IL-17 and IL-23 Cytokines in Immune-Mediated Diseases. *Annual Review of Medicine*. 2016;67:337-53.
7. Ciccia F, Guggino G, Rizzo A, Saieva L, Peralta S, Giardina A, et al. Type 3 innate lymphoid cells producing IL-17 and IL-22 are expanded in the gut, in the peripheral blood, synovial fluid and bone marrow of patients with ankylosing spondylitis. *Annals of the rheumatic diseases*. 2015;74(9):1739-47.
8. Leijten EF, van Kempen TS, Boes M, Michels-van Amelsfort JM, Hijnen D, Hartgring SA, et al. Brief Report: Enrichment of Activated Group 3 Innate Lymphoid Cells in Psoriatic Arthritis Synovial Fluid. *Arthritis & Rheumatology*. 2015;67(10):2673-8.
9. Villanova F, Flutter B, Tosi I, Grys K, Sreeneebus H, Perera GK, et al. Characterization of innate lymphoid cells in human skin and blood demonstrates increase of NKp44+ ILC3 in psoriasis. *Journal of Investigative Dermatology*. 2014;134(4):984-91.
10. Althoff CE, Sieper J, Song I-H, Haibel H, Weiß A, Diekhoff T, et al. Active inflammation and structural change in early active axial spondyloarthritis as detected by whole-body MRI. *Annals of the rheumatic diseases*. 2013;72(6):967-73.
11. Cuthbert RJ, Giannoudis PV, Wang XN, Nicholson L, Pawson D, Lubenko A, et al. Examining the feasibility of clinical grade CD271+ enrichment of mesenchymal stromal cells for bone regeneration. *PLoS One*. 2015;10(3):e0117855. PubMed PMID: 25760857. Pubmed Central PMCID: 4356586.
12. Xueyi L, Lina C, Zhenbiao W, Qing H, Qiang L, Zhu P. Levels of Circulating Th17 Cells and Regulatory T Cells in Ankylosing Spondylitis Patients with an Inadequate Response to Anti-TNF- α Therapy. *Journal of clinical immunology*. 2013;33(1):151-61.
13. El-Sherbiny Y, El-Zayadi A, Cuthbert R, Baboolal T, Fragkakis A, Jones E, et al. A4. 07 IL-22 impact on human bone marrow mesenchymal stem cells functions; a unique pathway that may contribute to aberrant new bone formation in human SPA. *Annals of the Rheumatic Diseases*. 2016;75(Suppl 1):A39-A40.
14. Reinhardt A, Yevsa T, Worbs T, Lienenklaus S, Sandrock I, Oberdörfer L, et al. IL-23-dependent $\gamma\delta$ T cells produce IL-17 and accumulate in enthesis, aortic valve, and ciliary body. *Arthritis & Rheumatology*. 2016.
15. Bernink JH, Peters CP, Munneke M, te Velde AA, Meijer SL, Weijer K, et al. Human type 1 innate lymphoid cells accumulate in inflamed mucosal tissues. *Nature immunology*. 2013;14(3):221-9.

FIGURE LEGENDS

Figure 1: Lymphocyte populations in enthesal tissue.

Schematic of the spine showing the area harvested for analysis (dotted line)(A). Photomicrograph of the enthesal region of the ACL stained with Haematoxylin and eosin (B). Lymphocyte populations in peripheral blood (PB, n=8, black bar), enthesal soft tissue (EST, n=3, white bar) and peri-enthesal bone (PEB, n=3, grey bar). Viable lymphocytes are classified as T-cells (CD3⁺), B-cells (CD19⁺) and NK-cells (CD3⁻, CD56⁺) cells outside of these categories are labelled "others" (C). T-cells (from C) subdivided into CD4⁺ (T-helper), CD8⁺ (cytotoxic T-cells), CD4^{neg}CD8^{neg} (double negative) and TCRγδ (γδ-Tcells) (D). Sorting strategy and representative plot for isolation of ILC subsets, ILC are identified from lymphocytes based on expression of CD127 and lack of expression of CD1a, CD3, CD14, CD11c, CD19, CD34, CD94, CD123, CD303, FCεR1, TRCαβ, TRCγδ. ILC subtypes were then identified; ILC1: CRTH2⁻ c-Kit⁻, ILC2: CRTH2⁺ c-Kit⁻, ILC3: CRTH2⁻ c-Kit⁺. ILC3s are subdivided based on expression of NKp44 (E). Proportion of lymphocytes identified as ILCs in PB (n=9), EST (n=7) and PEB (n=6) (F). Proportion of ILCs classified as ILC3s expressing the NKp44 marker in PB (n=8), EST (n=7) and PEB (n=6) (G). *p<0.05, **p<0.01, ***p<0.001 by Kruskal-Wallis test (C and D) and Mann-Whitney U test (F and G).

Figure 2: Phenotype confirmation and cytokine stimulation

Relative expression of *RORC* (*RORγt*) transcript in sorted ILC3 cells in comparison to unsorted mononuclear cells in enthesal soft tissue (n=6) (A) and peri-enthesal bone (n=5) (B). Expression of immunomodulatory transcripts ILC3s isolated from enthesal soft tissue (n=5, white circles), peri-enthesal bone (n=5, grey squares) and SpA synovial fluid (n=4, black triangles), line shows mean (C). Expression of *IL-23R* transcript in unsorted mononuclear cells and ILC3s (combined from both enthesal soft tissue and peri-enthesal bone both n=7, four values fell below detection in ILC3s), line shows mean, whiskers-standard error (D). Expression of *IL-17A* (E), *IL-17F* (F) and *IL-22* (G) in whole enthesal digests with and without stimulation by IL1β and IL-23 (all n=7). Triangles denote values below detection, these are given assumed values of 1x10⁻⁵, assumed values were also used for statistical comparison. All gene expression values shown are relative to *HPRT1* expression, *p<0.05, **p<0.01, by Man-Whitney U test, box plots show median (line), interquartile range (box) and extreme values (whiskers).

Figure 3: Tissue localisation in enthesal tissue.

Immunohistochemistry photomicrographs showing *RORγt* protein expression in ruptured Achilles tendon (A), as well as in osteoarthritic anterior cruciate ligament enthesal soft tissue (B), osteoarthritic anterior cruciate ligament peri-enthesal bone (C) and in regions of active bone remodelling in osteoarthritic anterior cruciate ligament (D). *RORγt* was mostly absent in spinous process enthesal soft tissue (E) but was expressed in spinous process peri-enthesal bone (F). Images are 200x magnification, arrows highlight regions of positive staining.

Supplementary Figure 1: Gating strategy for identification of $\gamma\delta$ T-cells

Lymphocytes were gated based on forward scatter (FSC) and side scatter (SSC) profile (A), live cells were then discriminated based on non-uptake of 7-Aminoactinomycin D (B). T-cells were identified based on expression of CD3 and CD45 (C) from these $\gamma\delta$ T-cells were identified by expression of T-cell receptor $\gamma\delta$ (TCR $\gamma\delta$) (D). Example shown, enthesal soft tissue.

Supplementary Figure 2: Immunofluorescence staining of normal human enthesis

Photomicrographs of human tonsil positive control and normal human enthesal soft tissue. Control human tonsil, blue – nucleus, red – CD3, green ROR γ t at 100x magnification, inset high power image (A). Enthesal soft tissue 100x magnification (B and C). High powered image showing accumulation CD3 positive T-cells (D).

Supplementary Table 1: Antibodies

Table shows all study antibodies FITC: Fluorescein, PE: Phycoerythrin, APC: Allophycocyanin, BV: Brilliant violet, BUV: Brilliant ultra-violet, Pcp: Peridinin chlorophyll protein, AF: Alexa fluor, FC: Flow cytometry, IHC: Immunohistochemistry, IF: Immunofluorescence. All antibodies for FC were used at manufacturers recommended concentrations.

Supplementary Table 2: ILC subpopulation frequency

Table shows ILC subtypes expressed as a percentage of total lymphocyte cellularity in enthesal soft tissue (EST, n=7) and peri-enthesal bone (PEB, n=6).

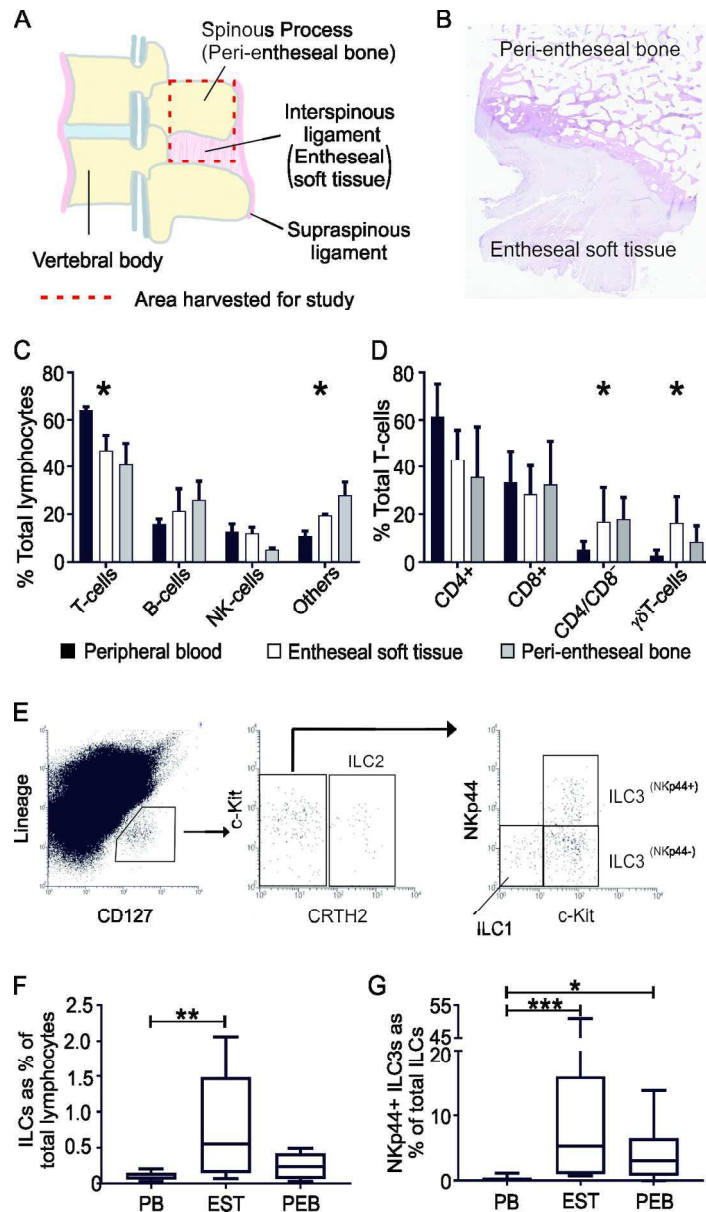


Figure 1: Lymphocyte populations in enthesal tissue.

Schematic of the spine showing the area harvested for analysis (dotted line)(A). Photomicrograph of the enthesal region of the ACL stained with Haematoxylin and eosin (B). Lymphocyte populations in peripheral blood (PB, n=8, black bar), enthesal soft tissue (EST, n=3, white bar) and peri-enthesal bone (PEB, n=3, grey bar). Viable lymphocytes are classified as T-cells (CD3+), B-cells (CD19+) and NK-cells (CD3-, CD56+) cells outside of these categories are labelled "others" (C). T-cells (from C) subdivided into CD4+ (T-helper), CD8+ (cytotoxic T-cells), CD4negCD8neg (double negative) and TCRγδ (γδ-Tcells) (D). Sorting strategy and representative plot for isolation of ILC subsets, ILC are identified from lymphocytes based on expression of CD127 and lack of expression of CD1a, CD3, CD14, CD11c, CD19, CD34, CD94, CD123, CD303, FCεR1, TRCαβ, TRCγδ. ILC subtypes were then identified; ILC1: CRTH2- c-Kit-, ILC2: CRTH2+ c-Kit-, ILC3: CRTH2- c-Kit+. ILC3s are subdivided based on expression of NKp44 (E). Proportion of lymphocytes identified as ILCs in PB (n=9), EST (n=7) and PEB (n=6) (F). Proportion of ILCs classified as ILC3s expressing the NKp44 marker in PB (n=8), EST (n=7) and PEB (n=6) (G). *p<0.05, **p<0.01, ***p<0.001 by Kruskal-Wallis test (C and D) and Mann-Whitney U test (F and G).

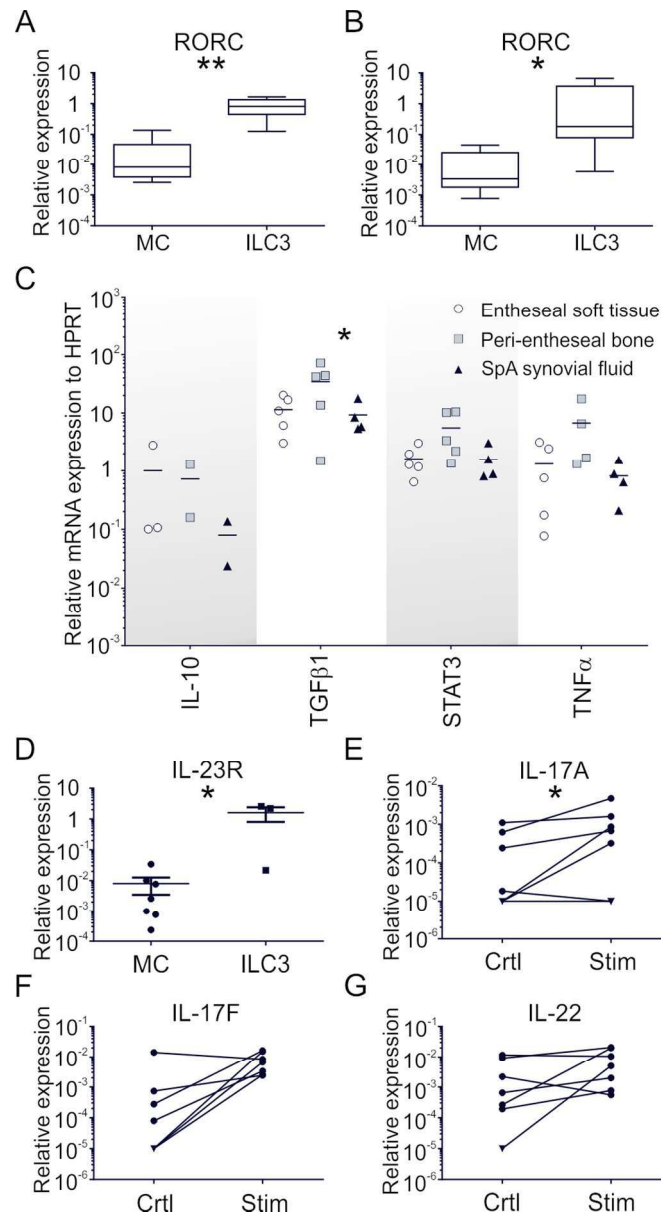


Figure 2: Phenotype confirmation and cytokine stimulation

Relative expression of RORC (ROR γ t) transcript in sorted ILC3 cells in comparison to unsorted mononuclear cells in enthesal soft tissue (n=6) (A) and peri-enthesal bone (n=5) (B). Expression of immunomodulatory transcripts ILC3s isolated from enthesal soft tissue (n=5, white circles), peri-enthesal bone (n=5, grey squares) and SpA synovial fluid (n=4, black triangles), line shows mean (C). Expression of IL-23R transcript in unsorted mononuclear cells and ILC3s (combined from both enthesal soft tissue and peri-enthesal bone both n=7, four values fell below detection in ILC3s), line shows mean, whiskers-standard error (D). Expression of IL-17A (E), IL-17F (F) and IL-22 (G) in whole enthesal digests with and without stimulation by IL1 β and IL-23 (all n=7). Triangles denote values below detection, these are given assumed values of 1x10⁻⁵, assumed values were also used for statistical comparison. All gene expression values shown are relative to HPRT1 expression, *p<0.05, **p<0.01, by Man-Whitney U test, box plots show median (line), interquartile range (box) and extreme values (whiskers).

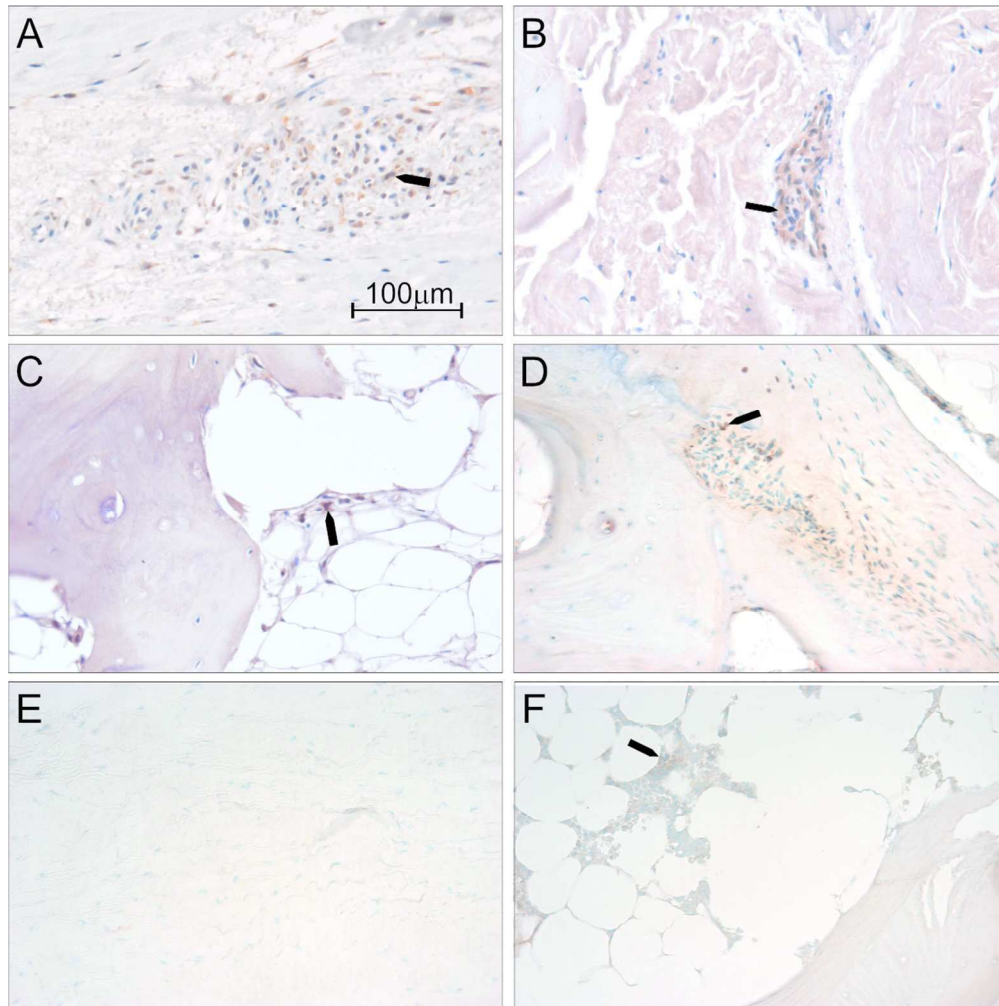


Figure 3: Tissue localisation in enthesal tissue.

Immunohistochemistry photomicrographs showing ROR γ t protein expression in ruptured Achilles tendon (A), as well as in the enthesal soft tissue (B), peri-enthesal bone (C) and in regions of active bone remodelling in osteoarthritic anterior cruciate ligament. ROR γ t was mostly absent in healthy enthesal tissue (E) but was expressed in healthy enthesal bone (F). Images are 200x magnification, arrows highlight regions of positive staining.